Kinetics and mechanism of gold anode corrosion in a weakly basic aqueous solution of triethylenetetramine

A. A. Laptev, M. D. Vedenyapina, V. V. Kuznetsov, S. A. Kulaishin, M. M. Kazakova, and E. D. Streltsova*

N. D. Zelinsky Institute of Organic Chemistry, Russian Academy of Sciences,
47 Leninsky prosp., 119991 Moscow, Russian Federation.
E-mail: mvedenyapina@yandex.ru

The electrochemical corrosion of a gold anode in a weakly basic aqueous solution of triethylenetetramine was studied. Scanning and transmission electron microscopy revealed the formation of a compact gold deposit on the cathode and gold nanoparticles in the electrolyte. The kinetics and mechanism of the corrosion of the gold anode were studied by gravimetry and cyclic voltammetry. The formation of colloidal gold particles in solution was established by transmission electron microscopy.

Key words: triethylenetetramine, cyclic voltammetry, gravimetry, gold electrode, corrosion, kinetics, colloidal gold.

A study of the electrochemical behavior of aliphatic diamines in weakly basic aqueous solutions of potassium carbonate on a gold electrode revealed corrosion of this anode followed by gold deposition on the cathode as a compact deposit.[1—10] In some cases, depending on the ligand type, formation of nano-sized colloidal gold particles in the electrolyte was observed. The ligands that were used include hexahydropyrimidine,[1] 1,5-diazabicyclo[3.1.0]hexane,[1,2] 6-methyl-1,5-diazabicyclo[3.1.0]hexane,[1,2] 6,6-dimethyl-1,5-diazabicyclo[3.1.0]hexane,[1,2] 1,3-diaminopropane,[3,4] 1,2-diaminopropane,[5] 2,2-dimethyl-1,3-diaminopropane,[6] ethylenediamine,[4,7] 1,4-diaminobutane,[8] 1-amino-3-(dimethylamino)propane,[9] and hexamethylenetetramine.[10] It was found that corrosion of the gold anode affords gold complexes with these ligands. These complexes are then reduced at the cathode to give a compact gold deposit or decompose in the electrolyte solution, thus forming gold nanoparticles.

Gold complexes with organic ligands are widely used in medicine,[11—14] in the chemistry of optical materials,[15] and in catalytic reactions.[16,17] The functional properties of the complexes are largely determined by the nature of ligands incorporated in the coordination sphere of the complexing ion.[18,19] Representatives of a new class of cyclometallated gold(III) complexes with benzopyridine, benzylpyridine, and 1,2-diaminocyclohexane (DACH) showed high antiproliferative activity.[18] The Au^{III}—DACH—ethylenediamine complexes with *cis*-, *trans*-, and *S*,*S*-positions of amino groups in DACH showed a cytotoxic activity *in vitro* against SGC7901 cancer cells; this activity proved to be higher than the activity of cisplatin.[19] A series of gold(III) complexes with various diamines, including aliphatic α,ω-diaminoalkanes, was synthesized and the structure and biological activity of the complexes were studied.[20] The stability of complexes depends on the ligand structure, while the gold electroreduction at the cathode is directly associated with electrolysis parameters. A part of gold is not deposited on the cathode, but migrates into the electrolyte solution to form a gold mirror or colloidal gold.[10] Thus, by selecting an appropriate ligand and parameters of electrolysis, it is possible to control the composition of the products of corrosion of a gold anode. Since colloidal gold is widely used in catalysis, nanoelectronics, nanophotonics, nanosensorics, cosmetology, and restoration works,[21—23] the search for new approaches to its preparation is still a relevant task.

This study addresses the mechanism and kinetics of corrosion of gold anode in weakly basic aqueous solutions of triethylenetetramine (TETA). A TETA molecule has four amino groups, two primary and two secondary ones. The molecule is acyclic and has a high chelating ability; TETA is used as a curing agent for epoxy resins, owing to its commercial availability and low cost.

Experimental

Commercial TETA (Acros) was used. Working solutions were prepared using doubly distilled water. Potassium carbon-

Published in Russian in *Izvestiya Akademii Nauk. Seriya Khimicheskaya,* No. 6, pp. 1158—1163, June, 2022.

1066-5285/22/7106-1158 © 2022 Springer Science+Business Media LLC

ate was of the analytically pure grade. The anodic corrosion of gold was studied in the galvanostatic mode in an undivided two-electrode cell. Gold and steel wires of 0.3 mm in diameter immersed into an electrolyte solution by 15 mm served as anode and cathode, respectively. The TETA concentration in a 0.05 *M* solution of K_2CO_3 was 1.0 mol L^{-1}; the volume of the working solution was 20 mL. The electrodes were weighed on an ABJ220-4NM electronic analytical balance (Kern, USA) ($d = 0.0001$ g) at certain intervals. Cyclic voltammograms were measured on a computer-controlled IPC Compact potentiostat in a three-electrode cell. A glass-sealed gold wire (99.99% Au) with a diameter of 0.3 mm and a length of 0.3 cm was used as the working electrode. A platinum wire of the same size sealed into glass served as the auxiliary electrode, and silver chloride reference electrode (Ag/AgCl/3*M* KCl) was used. A 0.05 *M* solution of K_2CO_3 with pH 11.1 was used as the supporting electrolyte. The concentration of TETA was 0.1 mol L^{-1}. In CV measurements, the potential sweep rate (v) was varied from 200 to 25 mV s^{-1}. The microstructure of the electrodes obtained after the electrolysis of gold in an aqueous solution of TETA was studied by field emission scanning electron microscopy (FE-STEM) on a Hitachi SU8000 electron microscope (Hitachi, Japan). The images were recorded in the secondary electron mode at an accelerating voltage of 2—30 kV and a working distance of 8.4—11.0 mm. The results of analytical measurements were optimized by the approach described previously.[24] The energy dispersive X-ray spectroscopic measurements were performed on an Oxford Instruments X-max energy dispersion spectrometer (UK). The cathode (steel wire) was placed on an aluminum stage of 25 mm in diameter for examination. The electrolyte obtained after completion of electrolysis and containing colloidal gold was analyzed by transmission electron microscopy (TEM) on a Hitachi HT7700 electron microscope (Japan). The images were recorded in the transmission (bright field) mode at an accelerating voltage of 100 kV. Prior to the measurement, the working solution was deposited on a thin carbon film attached to a copper grid of 3 mm in diameter. The grid was mounted in a special holder. The sample was deposited as a liquid and then dried *in vacuo*.

The product formed after completion of electrolysis was isolated by keeping the reaction solution in an open glass crystallization dish at room temperature until water completely evaporated. The resulting solid residue was extracted with methanol (2×10 mL), and the solution was concentrated *in vacuo*.

Results and Discussion

The mechanism and kinetics of corrosion of the gold anode were studied in a weakly basic solution of TETA using gravimetric analysis at a current of 10 mA for 15, 40, and 50 h. Like in our previous studies,[1—10] the experiments with TETA demonstrated corrosion of the gold anode with a weight loss and deposition of metallic gold on a steel cathode. Figure 1 shows the kinetics of corrosion over 40 h: loss of weight of the gold anode (m_{corr}, *1*); weight gain of the cathode deposit (m_{dep}, *3*); and weight of gold (m_{sol}) located in the working solution, which was calculated as the difference of m_{corr} and m_{dep} (*2*).

It can be seen from Fig. 1 that the anodic dissolution of gold (*1*) follows linear kinetics. As the duration of electrolysis increases, the increase in the cathode deposit weight and increase in the weight of gold in the electrolyte solution (m_{dep} and m_{sol}) deviate from the linear dependence. Curve *2*, which reflects the content of gold in the solution, passes through a maximum corresponding to the time of electrolysis of 27 h. This indicates that the cathodic deposition of gold becomes more intense than gold accumulation in electrolyte solution in the form of colloidal particles and complex compounds. After 40 h of the experiment, the content of gold in solution decreases more than threefold with respect to the electrodeposited gold. According to the data of Fig. 1, m_{sol} does not exceed 5 mg during the experimental time. In the beginning of the process (the first 5 h), the deposition of gold on the cathode is retarded. Apparently, during this period, a gold monolayer is formed on the steel cathode for the subsequent efficient deposition of gold from the complex.

The results of SEM and EDX examination of the steel cathode are depicted in Fig. 2. It can be seen in Fig. 2, *a* that the corrosion of gold anode is accompanied by the formation of a gold deposit in the form of spherical particles on the steel cathode surface. During corrosion of the gold anode, the weakly basic aqueous

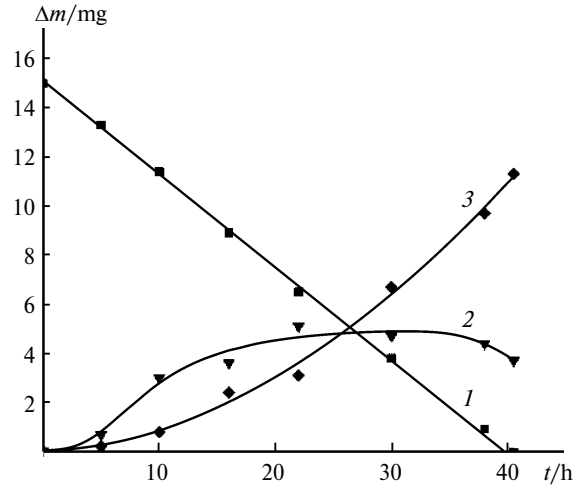

Fig. 1. Kinetics of anodic dissolution of metallic gold in an aqueous solution of TETA at a current of 10 mA and $C = 1.0$ mol L^{-1}; (*1*) weight loss of gold anode (m_{corr}); (*2*) calculated weight of gold (m_{sol}) in the solution; (*3*) weight of the cathodic deposit of metallic gold (m_{dep}) on the steel cathode.

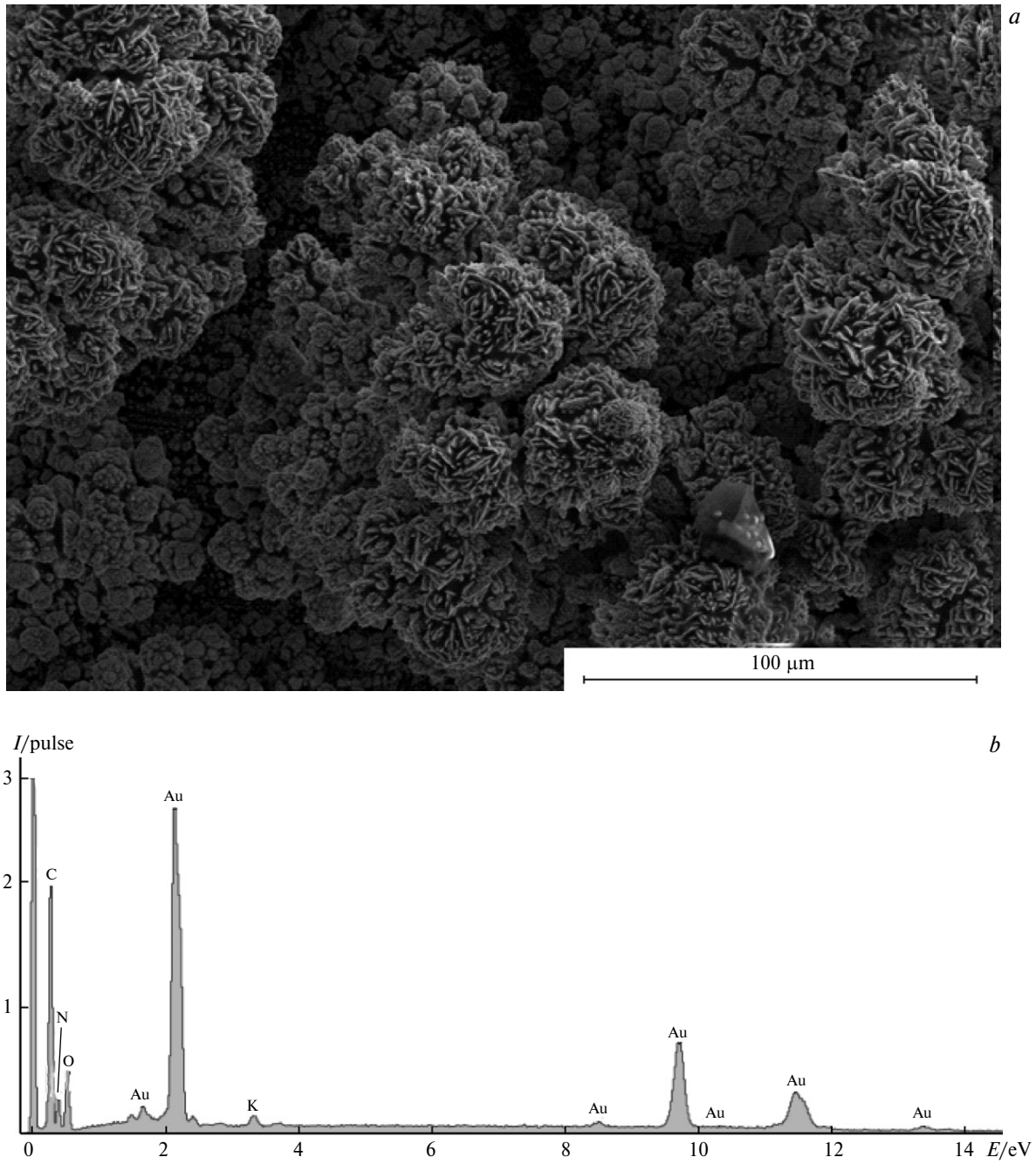

Fig. 2. Electron microscopic image of the gold deposit on the steel cathode (*a*) and results of EDX study of its chemical composition (*b*).

solution of TETA is colored pale yellow, and after 40 h of electrolysis, the color of the electrolyte solution becomes more intense.

A TEM study of the working solution showed that some colloidal gold particles were present after 15 h of electrolysis, while by the end of experiment (40 h), the amount of gold nanoparticles markedly increases and the nanoparticle size increases approximately 2-fold up to 5—10 nm (Fig. 3).

A comparison of the images shows that the size of colloidal gold particles formed after 15 h of electrolysis (3—7 nm) is smaller than the size of particles existing after 40 h of electrolysis (10—15 nm). The nanoparticles detected in the case of TETA were somewhat larger than those observed in the previously studied corrosion processes involving diamines.[1—10]

The kinetic patterns elucidated for anodic dissolution and cathodic deposition of gold can be analyzed,

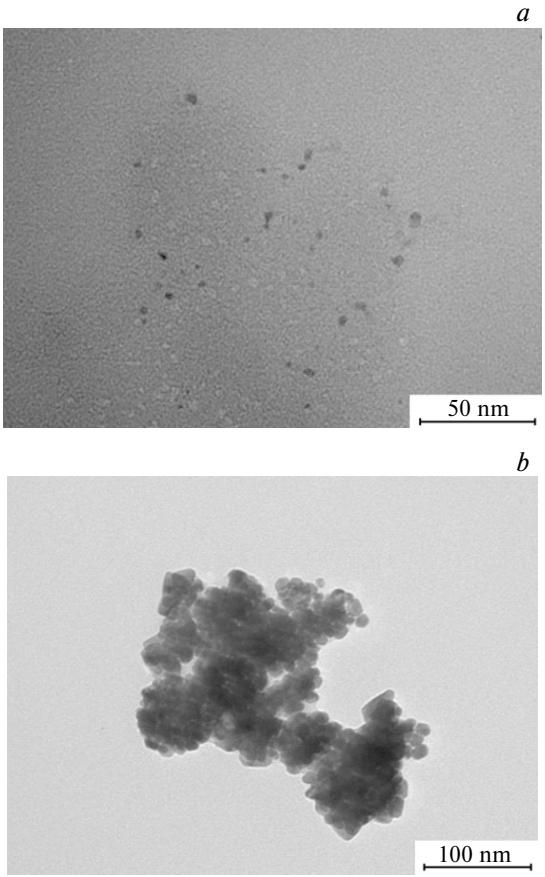

Fig. 3. Electron microscopic image of colloidal gold particles in the electrolyte after 15 (*a*) and 40 h (*b*) of electrolysis.

by analogy with previous studies,[1—10] using a system of differential equations:

$$dm_1/dt = k_1, \quad (1)$$

$$dm_2/dt = k_1 - k_2 m_2, \quad (2)$$

$$dm_3/dt = k_2 m_2, \quad (3)$$

where m_1, m_2, and m_3 are the weights of gold migrating from the anode to the solution, deposited from the solution on the cathode, and present in solution at time point t, respectively; k_1 is the rate constant of the anodic process; k_2 is the rate constant of the cathodic process. Solving this system of equations using the Mathcad software gave the values describing most accurately the experimental data: $k_1 = 0.371$ mg h^{-1}; $k_2 = 0.037$ h^{-1}. It can be seen that the rate of anodic dissolution is higher than the rate of cathodic process.

The cyclic voltammograms (CV) for the gold electrode in a weakly basic aqueous solution of TETA, which were recorded in the potential range from −100 to +1250 mV at different sweep rates, are shown in Fig. 4. The anodic branches of CV curves show weakly pronounced peaks in the potential range E = 500—1000 mV. It was shown that the intensity of these peaks increases with increasing potential sweep rate v. By analysis of the CV digital data, it is possible to determine, with some approximation, the maximum currents for all CV curves (see Fig. 4) and to draw conclusion about the shift of these values to more positive potentials. While recording several CV cycles, it was noted that responses in the anodic and cathodic branches are present in the first and subsequent cycles. This attests to the absence of strong adsorption of the substrate, resulting in the passivation of the anode surface. During the back sweep in the potential range E = 100—300 mV, the cathode branches show peaks, indicating reduction of the corrosion products.

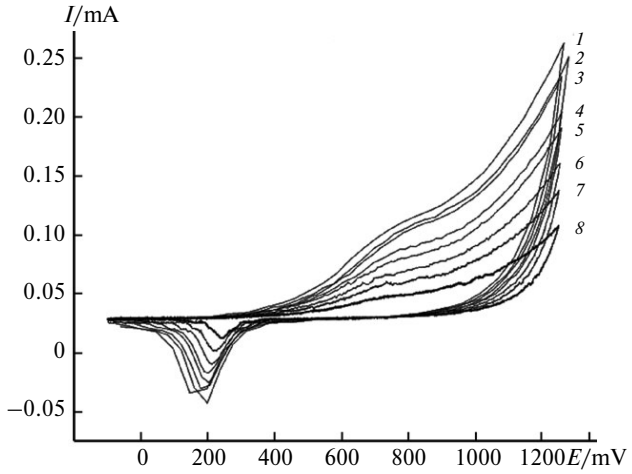

Fig. 4. Cyclic voltammograms in a weakly basic aqueous solution (0.05 M K_2CO_3) of TETA on Au electrode for various potential sweep rates: 200 (*1*), 175 (*2*), 150 (*3*), 125 (*4*), 100 (*5*), 75 (*6*), 50 (*7*), and 25 mV s^{-1} (*8*).

Table 1 summarizes the kinetic and electrochemical characteristics of the corrosion of gold anode in aqueous solutions of diaminoalkanes **1—5**. Analysis of the data of Table 1 provides the conclusion that the constants k_1 and k_2 for the anodic dissolution of gold and cathodic reduction of gold in TETA differ little from those in diaminopropane **1**. The dissolution rates of the gold anode during electrolysis in diaminopropane **1** and in TETA studied here are also similar.

The change in the electrochemical behavior of Au in solutions of diamines **1—5** may be due to both different electron densities on nitrogen atoms in these compounds and structural factors.

Thus, we studied for the first time the kinetics of gold anode corrosion in a weakly basic aqueous solution of TETA by gravimetric and CV methods. In line with

Table 1. Kinetic and electrochemical characteristics of the corrosion of gold anode in aqueous solutions of diaminoalkanes **1—5** at 10 mA

Compound	k_1 /mg h^{-1}	k_2[a]/h^{-1}	E_a[b]/mV	Dissolution rate /mg cm^{-2} h^{-1}	Reference
1	0.42	0.040	680	6.66	3, 4
2	0.55	0.110	572	8.73	4, 7
3	0.09	0.020	770	1.43	6
4	0.29	0.026	1125	4.58	9
5	0.37	0.037	—	5.88	This work

[a] Rate constant of reduction on the steel cathode.
[b] Maximum current potential in the anodic branch of CV curve.

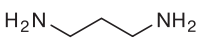

1,3-Diaminopropane (**1**)

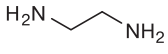

Ethylenediamine (**2**)

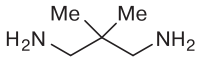

2,2-Dimethyl-1,3-diaminopropane (**3**)

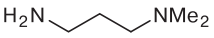

1-Amino-3-(dimethylamino)-propane (**4**)

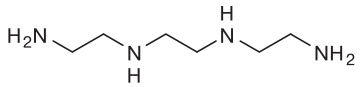

Triethylenetetramine (**5**)

the data published previously, the Au—TETA complex is formed and then reduced at the cathode to give a cathode deposit and colloidal gold in the electrolyte. Determination of the composition of the Au—TETA complex by elemental analysis of the electrolysis products indicates the presence of complexes containing one to three ligands. The study provides the conclusion that TETA has a high reactivity (according to the data of gravimetry) in the anodic dissolution of gold and in the electrochemical reduction of gold at the cathode.

We demonstrated for the first time the applicability of TETA, which is produced in industry on a large scale, for electrochemical redeposition of gold. It follows from gravimetric data that the reactivity of TETA in the electrochemical redeposition of gold is somewhat lower than that of the previously studied ethylenediamine; however, it is quite sufficient for the efficient use of TETA in this process. In addition, the possibility of preparing gold nanoparticles in an electrolyte solution deserves attention.

The authors are grateful to the Department of Structural Studies of the N. D. Zelinsky Institute of Organic Chemistry, Russian Academy of Sciences for electron microscopic examination of the samples.

No human or animal subjects were used in this research.

The authors declare no competing interests.

References

1. A. P. Simakova, M. D. Vedenyapina, V. V. Kuznetsov, N. N. Makhova, A. A. Vedenyapin, *Russ. J. Phys. Chem. A*, 2014, **88**, 331; DOI: 10.1134/S0036024414020241.
2. M. D. Vedenyapina, V. V. Kuznetsov, N. N. Makhova, A. A. Vedenyapin, *Russ. J. Phys. Chem. A*, 2016, **90**, 1903; DOI: 10.1134/S0036024416090284.
3. M. D. Vedenyapina, G. Ts. Ubushieva, V. V. Kuznetsov, N. N. Makhova, A. A. Vedenyapin, *Russ. J. Phys. Chem. A*, 2016, **90**, 2312; DOI: 10.1134/S0036024416110297.
4. M. D. Vedenyapina, V. V. Kuznetsov, D. I. Rodikova, N. N. Makhova, A. A. Vedenyapin, *Mendeleev Commun.*, 2018, **28**, 181; DOI: 10.1016/j.mencom.2018.03.024.
5. M. D. Vedenyapina, V. V. Kuznetsov, N. N. Makhova, D. I. Rodikova, *Russ. Chem. Bull.*, 2020, **69**, 1884; DOI: 10.1007/s11172-020-2974-5.
6. M. D. Vedenyapina, V. V. Kuznetzov, A. S. Dmitrenok, M. E. Minyaev, N. N. Makhova, M. M. Kazakova, *Russ. Chem. Bull.*, 2021, **70**, 735; DOI: 10.1007/s11172-021-3144-0.
7. M. D. Vedenyapina, V. V. Kuznetsov, N. N. Makhova, D. I. Rodikova, *Russ. J. Phys. Chem. A*, 2019, **93**, 466; DOI: 10.1134/S0036024419020304.
8. M. D. Vedenyapina, V. V. Kuznetsov, N. N. Makhova, D. I. Rodikova, *Russ. Chem.Bull.*, 2019, **68**, 1997; DOI: 10.1007/s11172-019-2658-1.
9. M. D. Vedenyapina, V. V. Kuznetsov, S. A. Kulaishin, N. N. Makhova, M. M. Kazakova, *Russ. J. Org. Chem.*, 2021, **57**, 1417; DOI: 10.1134/S1070428021090050.
10. M. D. Vedenyapina, S. A. Kulaishin, V. V. Kuznetsov, N. N. Makhova, M. M. Kazakova, *Russ. Chem. Bull.*, 2022, **71**, 52; DOI: 10.1007/s11172-022-3375-8.
11. B. Bertrand, A. Casini, *Dalton Trans.*, 2014, **43**, 4209; DOI: 10.1039/C3DT52524D.
12. T. Zou, C. T. Lum, C.-N. Lok, J.-J. Zhang, C.-M. Che, *Chem. Soc. Rev.*, 2015, **44**, 8786; DOI: 10.1039/C5CS00132C.
13. R. Visbal, V. Fernández-Moreira, I. Marzo, A. Laguna, M. C. Gimeno, *Dalton Trans.*, 2016, **45**, 15026; DOI: 10.1039/C6DT02878K.
14. C. Yeo, K. Ooi, E. Tiekink, *Molecules*, 2018, **23**, 1410; DOI: 10.3390/molecules23061410.
15. R. Czerwieniec, T. Hofbeck, O. Crespo, A. Laguna, M. C. Gimeno, H. Yersin, *Inorg. Chem.*, 2010, **49**, 3764; DOI: 10.1021/ic902325n.
16. M. Rudolph, A. S. K. Hashmi, *Chem. Soc. Rev.*, 2012, **41**, 2448; DOI: 10.1039/C1CS15279C.
17. M. Aliaga-Lavrijsen, R. P. Herrera, M. D. Villacampa, M. C.n Gimeno, *ASC Omega*, 2018, **3**, 9805; DOI: 10.1021/acsomega.8b01352.

18. S. Gukathasan, S. Parkin, S. G. Awuah, *Inorg. Chem.*, 2019, **58**, 9326; DOI: 10.1021/acs.inorgchem.9b01031.
19. S. S. Al-Jaroudi, M. Monim-ul-Mehboob, M. Altaf, A. A. Al-Saadi, M. I. M. Wazeer, S. Altuwaijri, A. A. Isab, *Biometals*, 2014, **27**, 1115; DOI: 10.1007/s10534-014-9771-2.
20. B. Petrovic, S. Radisavljevic, *Front. Chem.*, 2020, **8**, 379; DOI: 10.3389/fchem.2020.00379.
21. L. A. Dykman, N. G. Khlebtsov, *Russ. Chem. Rev.*, 2019, **88**, 229—247; DOI: 10.1070/RCR4843.
22. I. Saldan, O. Dobrovtseva, L. Sus, O. Makota, O. Pereviznyk, O. Kuntyi, O. Reshetnyak, *J. Solid State Electrochem.*, 2018, **22**, 637—656.
23. R. R. Fazleeva, G. R. Nasretdinova, Yu. N. Osin, A. Yu. Ziganshina, V. V. Yanilkina, *Russ. Chem. Bull.*, 2020, **69**, 241; DOI: 10.1007/s11172-020-2752-4.
24. V. V. Kachala, L. L. Khemchyan, A. S. Kashin, N. V. Orlov, A. A. Grachev, S. S. Zalesskiy, V. P. Ananikov, *Russ. Chem. Rev.*, 2013, **82**, 648; DOI: 10.1070/RC2013v082n07ABEH004413.

Received February 24, 2022;
in revised form March 31, 2022;
accepted April 12, 2022